Scratching resistance of SiC-rich nano-coatings produced by noble gas ion mixing

A.S. Racz, D. Dworschak, M. Valtiner, M. Menyhard

PII: S0257-8972(20)30144-4

DOI: https://doi.org/10.1016/j.surfcoat.2020.125475

Reference: SCT 125475

To appear in: *Surface & Coatings Technology*

Received date: 6 December 2019

Revised date: 12 February 2020

Accepted date: 14 February 2020

Please cite this article as: A.S. Racz, D. Dworschak, M. Valtiner, et al., Scratching resistance of SiC-rich nano-coatings produced by noble gas ion mixing, *Surface & Coatings Technology* (2020), https://doi.org/10.1016/j.surfcoat.2020.125475

Scratching Resistance of SiC-rich Nano-Coatings Produced by Noble Gas Ion Mixing

A.S. Racz [†ǁ],D. Dworschak[§], M. Valtiner [§], M. Menyhard[†]*

[†] Institute for Technical Physics and Materials Science, Centre for Energy Research, Hungarian Academy of Sciences, Konkoly Thege M. út 29-33, H-1121 Budapest, Hungary

[ǁ] Budapest University of Technology and Economics, Műegyetem rkp. 3, H-1111 Budapest, Hungary

[§] Institute for Applied Physics, Vienna University of Technology, Wiedner Hauptstrasse 8-10, A-1040 Vienna, Austria

ABSTRACT

SiC-rich nano-layers were produced at room temperature by applying ion beam mixing of various C/Si multilayer structures using argon and xenon ions with energy in the range of 40-120 keV and fluences between 0.25-3 x 10^{16} ions/cm^2. The mechanical behavior of the layers was characterized by scratch test. The scratching resistance of the ion mixed samples has been measured by standard scratch test applying an atomic-force microscope with a diamond-coated tip (radius < 15 nm) and they were compared to that measured on Si single crystal. The applied load varied in the range of 4-18 μN. The scratching resistance of the samples correlated with the effective areal density of the SiC; with increasing effective areal density the scratch depth decreases. Above sufficiently high effective areal density of SiC the scratch resistance (hardness) of the produced layer was somewhat higher than that of single crystal silicon. Previously it has been shown that such layers have excellent corrosion resistive properties as well. These findings allow to tune and design the mechanical and chemical properties of the SiC protective coatings.

KEYWORDS: *silicon carbide, nano-coating, ion beam mixing, atomic force microscopy, wear, scratch*

1. INTRODUCTION

Thin films serving as protective coatings in different environments are essentially important in various applications. Silicon carbide (SiC) is a material with many advantageous properties like biocompatibility, high heat resistance, high wear resistance, good thermal conductivity and inertness in corrosive environments. Due to these properties among others it is often used as a protective coating in harsh and also in biological environment [1–5]. A variety of techniques are available to produce SiC films, like physical vapor deposition (PVD) and atmospheric pressure chemical vapor deposition (CVD) [6,7]. Sha et al.[8] used RF plasma sputtering and a compound SiC target to deposit 160 nm thick SiC on porous Si substrate, after deposition the sample was annealed between 700-1000 °C. Zhao et al. [9] deposited β-SiC with various crystalline sizes on Si at 350 °C applying catalytic CVD. Daves et al. [10] applied plasma-enhanced CVD at 400 °C to deposit 250 nm thick amorphous SiC thin films and studied the deposition parameters on the film properties. Laboriante et al. [2] deposited 50 nm thick SiC on Si (100) using low pressure CVD at 780 °C. These above works applied elevated temperatures and the thickness of the produced SiC was mostly above 100 nm.

If high or medium temperature, because of the possible damage of the to be coated substrate, is excluded one should apply other (mainly non-equilibrium) methods for the production of the coating layer. Similarly the thickness of the coatings can be also important: for miniature applications e.g. M/NEMS systems, micromotors, bio-implants ultra-thin coatings are desirable due to reduced physical space between the substrate and the surface [11,12]. Recently it has been shown that ion bombardment induced mixing (IBM) could be a

good alternative to produce coatings with thicknesses below 100 nm at room temperature [13,14]. It has been reported that by applying (IBM) on C/Si multilayer structures the produced coatings exhibited excellent corrosion resistance properties [15]. Additionally it has been shown that this IBM can be described by TRIDYN simulation and consequently the corrosion resistance could be tailored by applying fast and cheap simulation techniques [16].

From the viewpoint of protective coatings besides the corrosion resistance the good mechanical behavior of the layer might be also important. As the thickness of the produced SiC-rich coatings was only some tens of nanometers conventional hardness tests are generally not suitable for testing. Alternatively a scratch test with an atomic force microscope (AFM) in which a tip is indented into the substrate and then moved at a fixed depth along the surface is applied for studying extreme thin layers [17]. It allows the sensing of tribological properties of hard coatings down to a deformation depth of several Å, thus, substrate related effects can be excluded [18]. E.g. Wienss et al. examined the scratching resistance of 100 nm thick magnetron sputtered diamond-like carbon coatings using AFM. They found a correlation between the hydrogen content in the film and the scratching resistance [19]. Wu et al. focused on the properties of B_4C films thinner than 20 nm deposited by magnetron sputtering. A correlation was established between the compressive residual stress present in the films and the scratching resistance [20]. Beake et al. performed scratch tests on 5-80 nm thick tetrahedral amorphous carbon (ta-C) films deposited on silicon where they determined the critical load for failure in different layer thicknesses. Thicker coatings provided higher critical load [21]. Tangpatjaroen et al. investigated 500 nm thick nanocrystalline (nc) SiC films produced by chemical vapor deposition (CVD). They have shown that the scratching resistance of SiC compared to Si depends on the size of the contact [22]. It has been also shown that the deformation during scratching is size dependent which makes the evaluation difficult [23,24]. The scratch depth provided by the scratch test experiment in many cases can

be directly used to determine the wear resistance of the material studied, and additionally this phenomenological parameter in many cases is connected to such basic material parameters like hardness and friction coefficient [22,25,26].

Herein, we report on the scratching tests of SiC-rich nano-coating layers produced by ion mixing at room temperature. The coating layers were produced by applying various noble gas irradiation parameters on various multilayer structures consisting of C (10 nm) and Si (20 nm) layers on a Si substrate resulting in SiC-rich layers of various distributions. The scratch resistance was measured by AFM in combination with a diamond-coated-tipped cantilever. We will show that the previously introduced effective areal density of SiC [15], which is in good correlation with the corrosion resistance of the layer, also correlates with the scratching resistance of the samples. Sufficiently high effective areal density of the irradiated sample resulted in a scratch resistance somewhat higher than that of single crystal silicon.

2. EXPERIMENTAL SECTION

2.1 Production of SiC-rich layer by means of IBM

It has been shown previously that ion bombardment induced mixing (IBM) of layer systems containing pure C and Si layers may result in formation of SiC rich layer [13,15]. The actual SiC concentration distribution along the depth depends on the conditions of the IBM and the initial layer structure.

For producing various SiC in-depth distributions two different multilayer structures were irradiated by argon and xenon ions at room temperature. The structures C (10nm) /Si (20nm) /C (10nm) /Si (20nm) /C (10nm) / single-crystal Si-substrate and Si (20nm) /C (10nm) /Si (20nm)/C (10nm) / single-crystal Si-substrate were produced by sputtering; the

deposited layers were amorphous [14]. For easier reference the first structure will be called as 10-20, the latter one as 20-10 sample.

The applied fluences were between 0.25-3 x 10^{16} ion/cm^2, and the projectiles were Ar^+ (40 keV) and Xe^+ (120keV). The Ar^+ irradiations took place in a Varian-type ion implanter. The angle of incidence was 7° with respect to the surface normal. The ion beam current density was 0.4 μA/cm^2. The Xe^+ irradiation was performed in the Heavy Ion Cascade Implanter of the Institute for Particle and Nuclear Physics of the Wigner Research Centre for Physics in Budapest. The ion beam current density was 0.75 μA/cm^2. In both cases the ion beam with typically millimeter dimensions was x–y scanned across the full sample surface (1-2 cm^2) in order to achieve good irradiation homogeneity within the exposed area. In both cases the heating effects are negligible.

2.2 AES depth profiling

The concentration distribution along the depth of the target components and the projectiles before and after the ion irradiation has been determined by AES depth profiling. The Auger spectra were recorded by a STAIB DESA 150 pre-retarded Cylindrical Mirror Analyzer (CMA) in direct current mode. 1 keV Ar^+ ions were used for the AES depth profiling with an angle of incidence of 80º with respect to the surface normal. To avoid heating effects a mild ion sputtering has been applied; the removal rate was about 0.2 nm/s. This was achieved by applying an ion beam current of about 4 μA/mm^2. One etching step lasted only 20 s. The ion current was kept constant during sputtering. The sample was rotated (6 rev/min) during ion bombardment. These parameters were chosen to minimize the ion bombardment-induced surface and interface morphology changes [27].

The detailed description of the AES evaluation is described elsewhere [15]. Summarizing; the measured C (KLL) Auger peak could be decomposed into graphitic and

carbide components. The relative sensitivity factor method for the calculation of the atomic concentrations has been applied [28]. The sputtering time was transformed to removed thickness for getting depth profiles [29]. Hence, the AES analysis provided the in-depth distributions of Si, C, SiC and Ar or Xe.

2.3 Scratch test

The AES depth profiles have shown that in the majority of the cases not the whole upper carbon layer was consumed by the IBM-induced compound formation. Therefore the SiC-rich region was covered by a carbon layer of various thicknesses. Before the scratch test this layer was removed by oxidation in microwave plasma for 10 min, which did not affect the SiC present [30]. The surface topography and the scratch resistance was investigated by an AFM (MFP-3D, Asylum Research, CA) applying a diamond-coated tip (tip radius < 15 nm) mounted on a stainless steel cantilever. Due to the high sensitivity and small tip radius, the diamond-coated tip was able to obtain surface morphology and to create constant-force scratches in the surface. Each sample received parallel scratches with 9 different normal forces systematically increasing from 4.6 μN to 17.4 μN, the testing forces were equally spaced in the range. The applied loading force was derived from the bending of the actual cantilever and its spring constant measured by thermal noise. The following procedure for each measurement has been applied. *a./* Imaging of the area, *b./* Creation of 1 μm long scratches with the preset force, the sliding speed was 800 nm/sec *c./* Imaging of the area of the scratches with the same tip. The images were evaluated by applying Gwyddion [31] software. The scratch depth was calculated over several scan lines and averaged.

3. RESULTS

3.1 SiC concentration distribution of the samples

The effects of the noble gas irradiation were studied thoroughly previously [8,9] , it has been shown that the in-depth distribution of the formed SiC could be tailored by varying the ion energy, fluence and the layer structure. For better understanding AES depth profiles of a 10-20 pristine and a 40 keV, 0.25 x 10 ^{16} Ar^+/cm^2 irradiated sample are provided in Fig. 1 a and b. We can see in Fig. 1a that there are only pure carbon and silicon layers and all interfaces are sharp. The effect of irradiation is depicted in Fig. 1b which shows the depth profile of a 40 keV, 0.25 x10^{16} Ar^+/cm^2 irradiated sample. It is presented that due to IBM the layer structure altered and a mixture of SiC, Si and C forms. The SiC began to grow from the interfaces and its concentration varies along the depth.

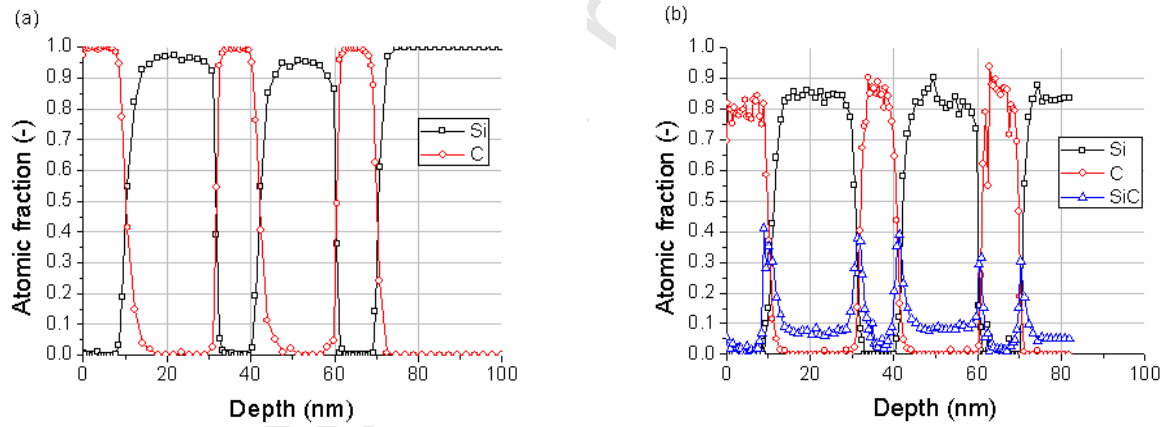

Fig. 1. AES depth profiles of the 10-20 sample a. pristine and b. irradiated (0.25 x10^{16} Ar^+/cm^2, 40keV).

Fig. 2 shows that by varying the applied fluence and energy the depth distribution of SiC strongly changes. Fig. 2a presents the depth profile of a 40 keV, 3 x $10^{16}Ar^+/cm^2$ irradiation on a 10-20 sample while Fig. 2b the depth profile of a 20-10 sample after irradiation of 120 keV, 3 x 10^{16} Xe^+/cm^2. In the case of argon irradiation the higher fluence, compared to Fig. 1b, resulted in overlapping of the intermixed regions growing from neighboring interfaces. In

the case of the higher energy xenon irradiation (projected range 55±12 nm [32]) the same fluence as in the case of argon (projected range 43±14 nm [32]) caused a quasi continuous homogeneous SiC distribution since in the case of xenon the second interface is more affected by ion mixing than in the case of argon. These examples clearly show that a great variety of SiC in-depth distribution can be produced by varying the irradiation parameters and layer structure.

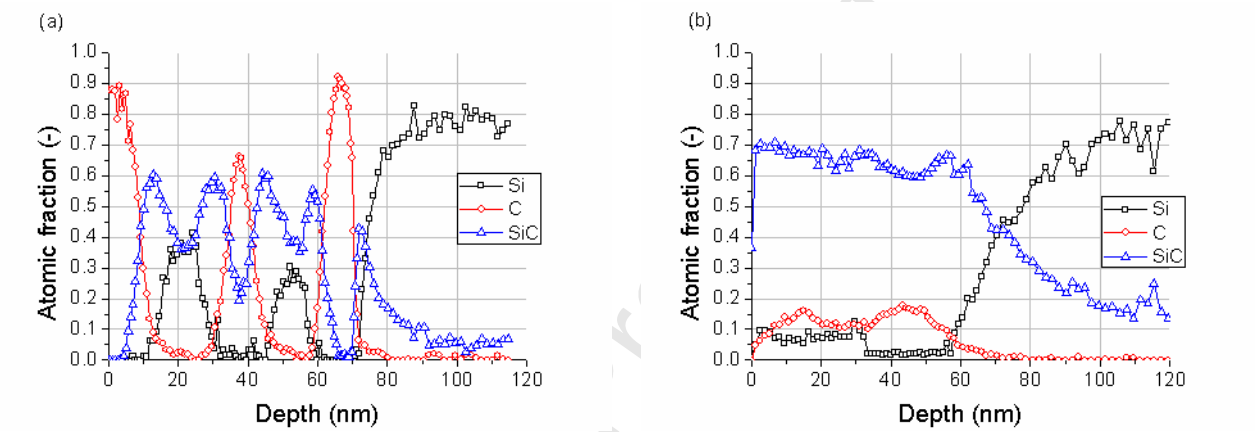

Fig. 2. AES depth profile recorded after a. 40 keV, 3 x 10^{16} Ar^{+}/cm^{2} irradiation of 10-20 sample b. 120 keV, 3 x 10^{16} Xe^{+}/cm^{2} irradiation of 20-10 sample.

Varying the irradiation conditions results in various SiC distributions along the depth. The quantification of these SiC distributions is not straightforward, especially because the concentration varies along the depth. For the easier handling of the SiC in-depth distribution and quantifying the amount of SiC produced the term areal density can be used, which is frequently applied in the case of IBM. It is the integral of an element, compound along the depth which gives the total amount of the chosen element, compound in the sample [33]. In our previous works, which dealt with the chemical resistance of the ion mixed layer against harsh chemical effects [15] we have introduced the term effective areal density of SiC which was defined as the integral of the concentration of SiC from that depth where its amount is

higher than 20% until that depth where its concentration goes below 20% again [15]. This was based on the experimental observations that good chemical resistance was connected to a certain SiC concentration. Table 1 summarizes the SiC effective areal density values of the samples studied by scratch test. They were calculated from the AES depth profiles by addition of the removed atoms from that depth where the SiC concentration is higher than 20% until that depth where its concentration goes below 20% again. This means that for irradiation 40 keV, 0.25 x 10^{16} Ar^+/cm^2 (Fig. 1b) the profile was integrated only between 9 and 13 nm. At the same time for irradiation 40 keV, 3 x 10^{16} Ar^+/cm^2 (Fig. 2a) the SiC concentration was mainly above 20%, therefore the profile was integrated between 7 and 63 nm.

Table 1. Summary of the SiC effective areal density values for different irradiations on different layer structures

Layer structure	*Irradiation conditions*	*Effective areal density (Si-C bond/ nm^2)*
10-20	0.25 x 10^{16} Ar^+/cm^2	71
	0.5 x 10^{16} Ar^+/cm^2	340
	1 x 10^{16} Ar^+/cm^2	576
	3 x 10^{16} Ar^+/cm^2	1554
	0.25 x 10^{16} Xe^+/cm^2	521
	0.5 x 10^{16} Xe^+/cm^2	1100
	1 x 10^{16} Xe^+/cm^2	1727
20-10	3 x 10^{16} Xe^+/cm^2	1826

3.2 Scratch test

The irradiated specimens and a single-crystal silicon have been tested with 9 equally spaced forces in the range of 4.6-17.4 μN. A typical measurement is depicted in Fig.3. Fig. 3 a-c shows the AFM images with the corresponding height profiles of the scratched a. 10-20 sample after 3 x 10^{16} Ar^{+}/cm^{2} irradiation, b. Si substrate and c. 10-20 sample after 0.25 x 10^{16} Ar^{+}/cm^{2} irradiation, for normal loads 9.4; 12.6 and 15.8 μN (the load increases from left to right). The line profiles clearly show that the scratch depths are different; the highest is for sample 10-20 irradiated by 0.25 x 10^{16} Ar^{+}/cm^{2} then comes the silicon single crystal, while the sample 10-20 with irradiation of 3 x 10^{16} Ar^{+}/cm^{2} shows the highest scratch resistance (lowest scratch depths). It should be emphasized that the observed trend does not depend on the applied load. It can be also seen that the groove depth is below 1 nm which is far below the 10% of the overall layer thickness therefore the mechanical properties can be considered as layer dominated.

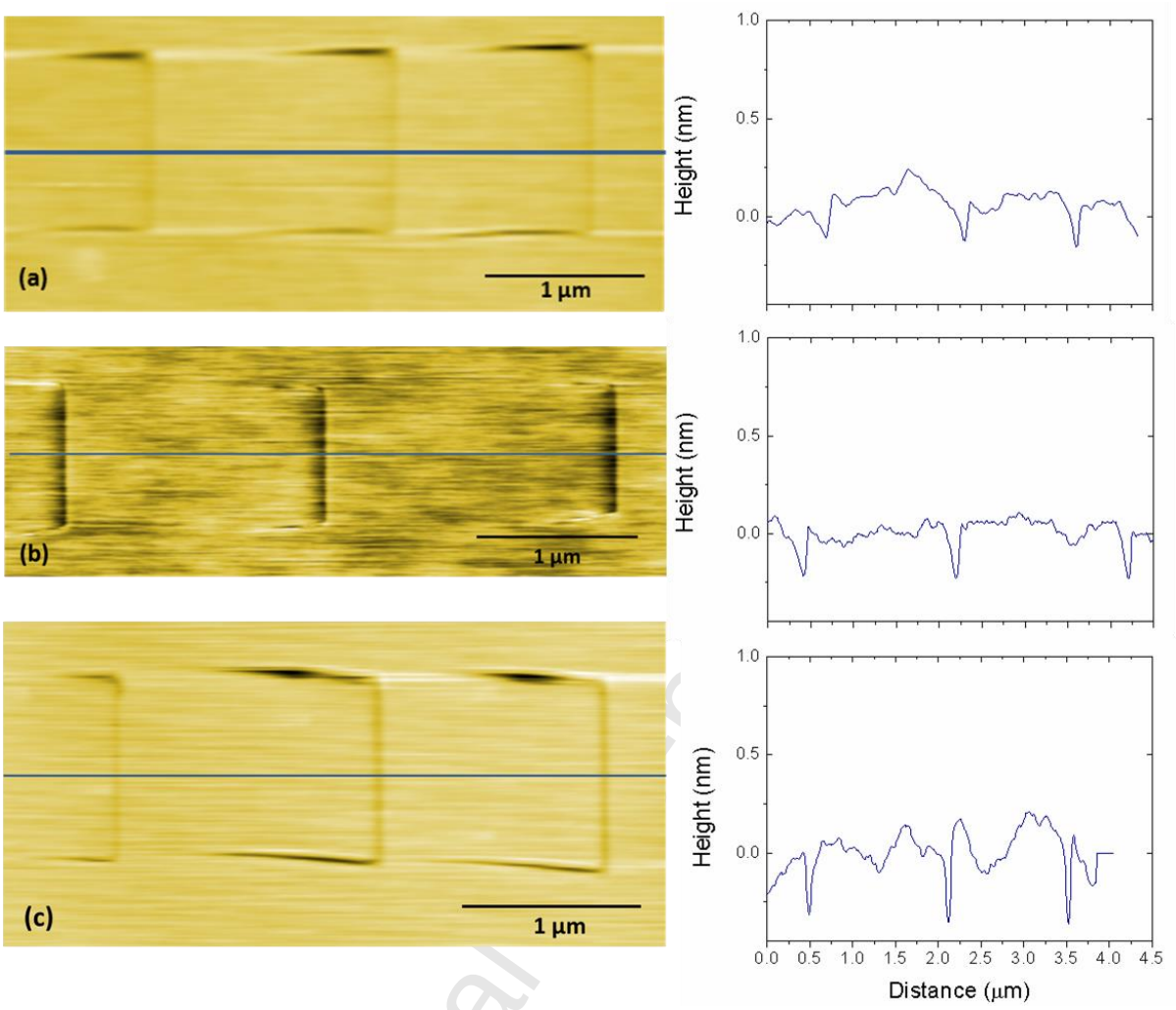

Fig. 3. AFM images with the corresponding height profiles of scratch tests performed over 9.4; 12.6 and 15.8 µN normal loads (the loads are increasing from left to right) using a diamond-coated AFM tip sliding on: a. 40 keV, 3 x 10^{16} Ar^{+}/cm^{2} irradiated 10-20 sample; b. single crystal Si; c. 40 keV, 0.25 x 10^{16} Ar^{+}/cm^{2} irradiated 10-20 sample.

4. DISCUSSION

All the results, the experimentally measured scratch depth vs applied load curves for all samples are summarized in Fig. 4; the parameters are the irradiation conditions. The trends are clear, the scratch depth measured on a given sample increases (after a threshold) up to a saturation value, which remains constant during further increase of the load. Our primary

interest is, however, to reveal dependence of the scratch resistance on the amount of SiC produced; this dependence needs another representation.

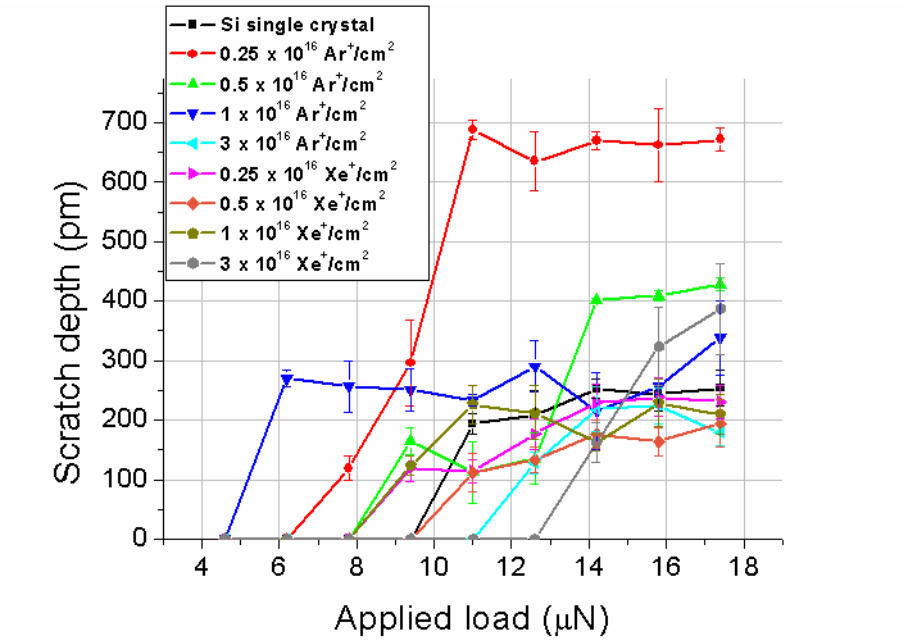

Fig. 4. Scratch depth vs. applied normal loads for all irradiated samples and the silicon single crystal.

Our previously introduced effective areal density of SiC showed a good correlation with the chemical resistance of the samples. In the present case it will be checked whether the same quantity can be used for the mechanical characterization of the samples after irradiation. Note that the scratch test (the additional carbon layer which covered the SiC-rich region had been removed before the test) because of its low penetration depth measures the mechanical behavior of the region determined by the effective areal density, that is, that region which is responsible for the good chemical resistance. The effective areal density values calculated in this experiment for the different irradiations were summarized in Table 1.

Fig. 5 shows the scratch depth vs effective areal densities; the parameter is the applied force (a. 9.4; b. 12.6 and c. 15.8 μN). The effective areal density even for the case of mechanical properties seems to be a meaningful parameter. There is a general trend: with

increasing effective areal density, that is, with increasing amount of SiC (consequently increased thickness of the SiC-rich layer) the scratch depth generally decreases down to a saturation value. Further increase of the SiC amount does not lead to significant improvement of the scratch resistances. This general behavior is somewhat obscured by some additional parameters. We observe that at low applied loads (Fig. 5a) at high effective areal densities, above 1000 Si-C bond/nm^2 from the three measured values two (for 1100 and 1826 Si-C bond/nm^2) is 0, which means that our load is lower than the threshold value. It fits the trend since with increasing effective areal density the scratch resistance increases and accordingly the threshold is higher than the applied load. At 1727 Si-C bond/nm^2 effective areal density well measurable scratch depth was obtained; this behavior might be explained that the threshold has some scatter and being close to it, scratch forms or does not form. This explanation is supported by the measurements at higher loads of 12.6 and 15.8 μN. At 12.6 μN load we are always above the threshold except the highest 1826 Si-C bond/nm^2 effective areal density, while at 15.8 μN load we are always above the threshold. These observations allow to make rough estimates of the threshold values for the various effective areal densities. The threshold value for making scratch is about 10 and 13 μN, for effective areal density of 1100 and 1826 Si-C bond/nm^2, respectively. These rough estimates also fit to the general trend; higher effective areal density higher threshold. At the highest load of 15.8 μN we are always above the threshold; in this case a quasi stationary value of the scratch depth is reached.

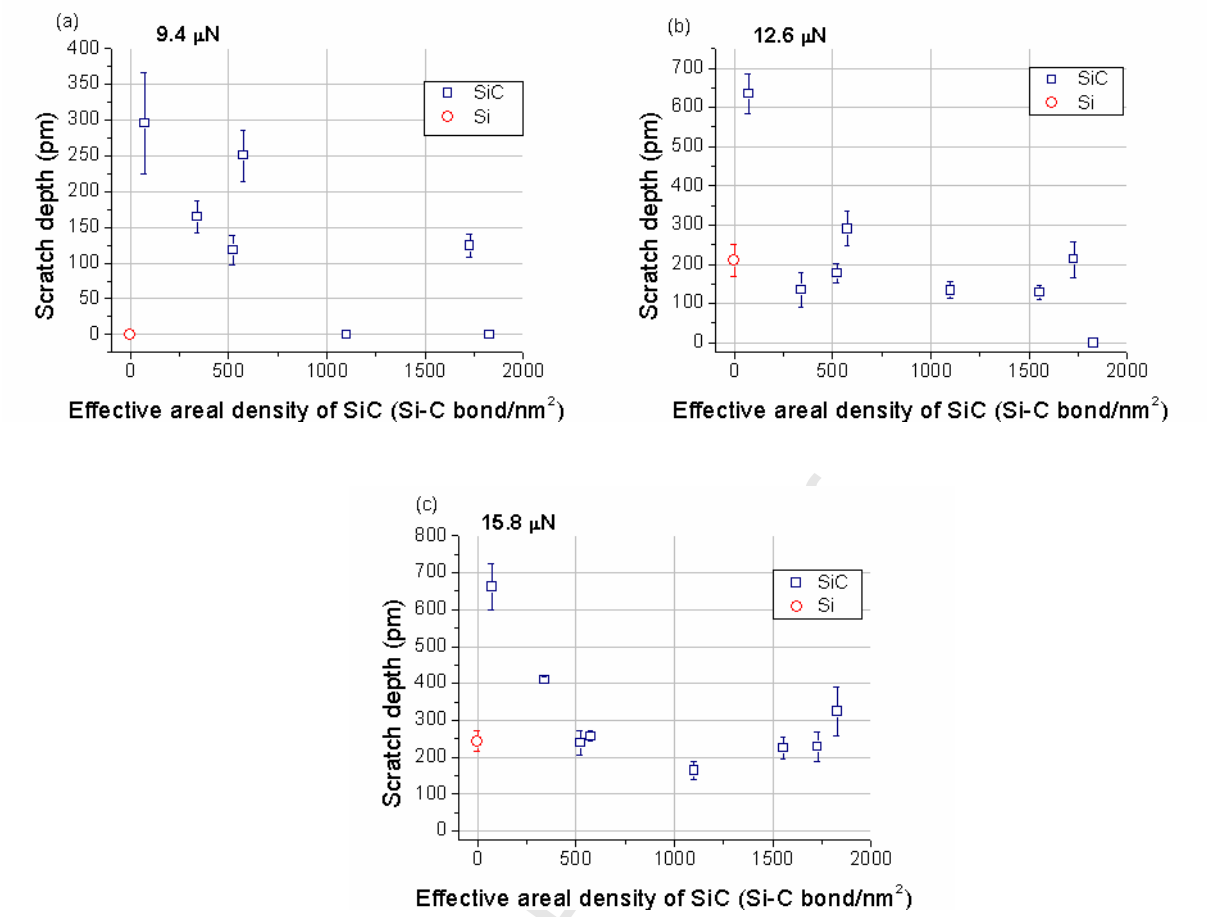

Fig. 5. Scratch depth vs the effective areal density of SiC for normal loads of a. 9.4 b. 12.6 and c. 15.8 µN (the scratch depth measured on the silicon substrate is also provided).

The scratch test is a relatively easy measurement; one should simply scratch the material and measure the scratch depth, which in principle can be directly connected to the wear resistance of the material [22,26,34]. It turns out, however, that the scratching process is a rather difficult one and one must be cautious with interpreting the results. If the scratching device, tip, is not sharp and the applied load is not too low, then the majority of the work made by the load while creating the scratch is used for plastic deformation. In this case the wear resistance is proportional to the hardness of the given material, *H* [35]. It means that a simple equation, namely the Archard equation [36] connects the experimentally easily

measurable scratch depth to a real material parameter of hardness. The equation (eq 1) reads as

$$H=\frac{kWx}{V} \qquad (1)$$

where, V is the volume of material removed, k is a dimensionless wear coefficient, W is the normal load, x is the sliding distance, and H is the hardness of the softer of the two contacting materials using a diamond tip generally the studied material. Eq. 1 provides easily measurable data for determining the hardness of the material.

Tangpatjaroen et al. however, have shown that this simple picture breaks down by applying sharp tester and low load [22]. They have studied the wear resistance of single and nano crystal SiC-s with respect to Si. Using a Berkovich diamond tip with a radius of 370 nm and applied load in the range of 50 - 2000 μN, the expected results have been obtained; the scratch depths for the SiC materials were less than that measured on Si according to the above equation; the higher hardness of SiC results in shallower scratch. On the other hand if they used a tip with radius of 15 nm and applied load in the range of 120 nN-3.5 μN an unexpected result has been obtained; the scratch depth of the harder material (SiC) became higher than that of the softer (Si) material. This behavior was explained by the higher weight of the friction which means that friction dominates plastic deformation.

In our experiment similar diamond tip with the same radius has been applied but the applied load range was somewhat higher, 5-17 μN, than that of Tangpatjaroen et al. [22] The question arises which process is valid for our case, whether the plastic deformation or the friction process is dominating? Considering Fig. 5 it can be seen that with the increase of the effective areal density, with the increase the amount of SiC in the surface close layer, the scratch depth decreases. This behavior can be easily explained by eq 1 which tells that the

scratch depth is inversely proportional to the hardness, assuming that the hardness of the composite material scales with the amount of SiC. If the friction process determines the scratch depth then we should consider that based on Tangpatjaroen et al. [22] the interfacial strength of the Si is higher than that of SiC which caused the strange result. In our case the amount of unreacted Si decreases with increasing effective areal density and the increase of the scratch depth is expected. Since the experimental results are just contrary we conclude that at our higher loads the scratch depth is inversely proportional to the hardness.

The SiC has various polytypes; in bulk form all of them are hard with a hardness in the range of 33 ±5 GPa. It is also known that the hardness of the micro and nano crystalline SiC layer is even higher than that of the bulk SiC, being in the range of 40 GPa. The hardness of bulk Si is around 10 GPa, that is much lower. Though the hardness measured on thin films generally differ from that of bulk still the above relation prevails for the thin films made of Si and SiC. In the case of SiC and Si thin films the hardness strongly and weakly depends on the way of preparation, respectively. Namely, in the case of SiC the hardness varies (depending on the deposition parameters used for thin film production) in the range of 25-50 GPa while in the case of Si this range is much lower 8-12 GPa [37,38]. It should be emphasized, however, that we have not found, hardness data for real thin layers of either material. Thus, for qualitative comparison of the hardness values we will use the Si single crystal (exhibiting well defined hardness value) sample for reference.

Considering the change of the scratch depth vs effective areal density (Fig. 5) we conclude that up to about 1000 Si-C bond/nm^2 effective areal density the scratch depth decreases with increasing areal density, while above this value remains constant. The qualitative explanation of the first region of the curves is simple; the effective areal density increases, the ratio of SiC/Si increases that is, the relative weight of the harder SiC increases

thus, the scratch depth should decrease. Afterwards above 1000 Si-C bond/nm^2 the hardness of the intermixed layer is not increasing any more, it reached a stationary value.

Comparing the scratch depths obtained from the ion irradiated sample with that of Si it can be seen that at the lowest areal density independently from the applied load the scratch depth is anomaly high, that is the hardness is extremely low; the scratching depth is larger than that value measured at pure Si, respectively. This low value can be explained by the fact that in these samples low argon fluence irradiation results in a very low SiC production (see Fig. 1b). Practically we are measuring the mechanical properties of the non-irradiated sample, that is, the behavior of the first amorphous Si layer on a soft graphitic carbon layer. Based on this result we conclude that the hardness of this system is rather low. On the other hand in the case of high SiC effective areal densities (> 1000 Si-C bond/nm^2) the scratching depth is lower or approximately the same than that value measured at pure Si, therefore the hardness of the ion mixed layers is equal or higher than 12 GPa.

Concluding applying proper irradiation parameters the hardness of the irradiated samples approximates the properties of the single-crystal silicon. Though these hardness values are lower than that of the SiC, they are still sufficient for certain applications and by varying the film structure and parameters of irradiation it can be tailored according to the demand.

Previously the corrosion behavior of the ion mixed layers has been measured, as well [15]. Potentiodynamic corrosion test has been performed in an electrochemical three-electrode glass cell in 4M KOH solution. The corrosion current densities were obtained by Tafel extrapolation from the polarisation curves from which the corrosion rates were calculated by Faraday's law. It is interesting to compare the corrosion and the scratch

resistance of the samples. Fig. 6 shows together the corrosion rates and the scratch depths in function of the SiC effective areal density values for all samples.

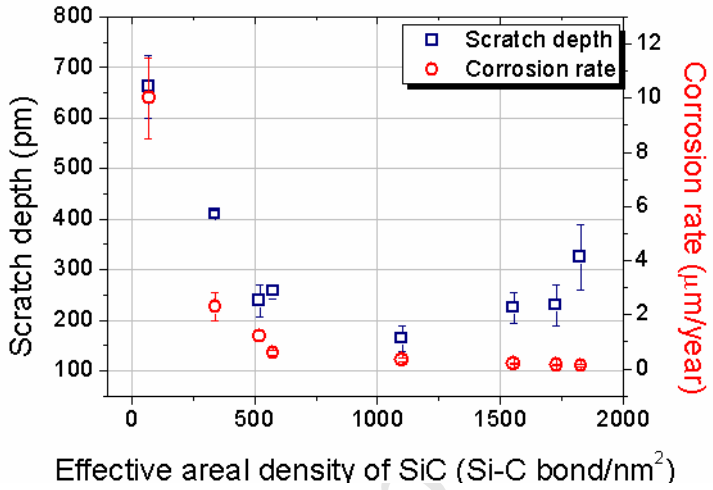

Fig. 6. Scratch depth and corrosion rate vs the effective areal density of SiC for all samples for normal load 15.8 μN.

The shapes of the two curves are surprisingly similar, even the points at low areal densities behaves similarly. It means that the two quantities, corrosion resistance and scratch resistance (hardness) depends on a similar way on the amount and distribution of the SiC. Consequently if either of them is tuned according to some demand the other simultaneously changes as well. The advantageous consequence of this behavior is that if we prepare a layer with high chemical resistance its wear resistance will be high as well.

5. CONCLUSIONS

Various C/Si multilayers were irradiated by Ar^+ and Xe^+ ions with energy in the range of 40-120 keV producing SiC-rich layers of various concentrations and distributions at room temperature. The scratch resistance of the irradiated sample together with a Si single crystal have been measured by standard scratch test applying an AFM with a diamond-coated tip (radius < 15 nm). The applied load varied in the range of 4-18 μN. The scratch resistance of

the irradiated sample correlated with the effective areal density of the SiC; with increasing effective areal density the scratch depth decreased. By using the results obtained on single crystal Si the hardness of the irradiated sample was estimated; it turned out that the hardness of the SiC-rich layers is similar to that of Si if their effective areal density is higher than 1000 Si-C bond/nm^2. It has been also shown that the chemical resistance of the ion mixed layer correlates with its hardness; if we prepare a layer with high chemical resistance its wear resistance will be automatically high, as well. The results enable the tailoring of the mechanical and chemical properties of SiC nano-coatings which could be served as protective layers in harsh environments.

AUTHOR INFORMATION

Corresponding Author

*E-mail: menyhard.miklos@energia.mta.hu

ACKNOWLEDGEMENT

The authors thank for the support of Ernst-Mach Scholarship of the OEAD (Österreichischer Austauschdienst) and the Austrian-Hungarian Foundation.

REFERENCES

[1] X. Lei, S. Kane, S. Cogan, H. Lorach, L. Galambos, P. Huie, K. Mathieson, T. Kamins, J. Harris, D. Palanker, SiC protective coating for photovoltaic retinal prosthesis, J. Neural Eng. 13 (2016) 046016. https://doi.org/10.1088/1741-2560/13/4/046016.

[2] I. Laboriante, A. Suwandi, C. Carraro, R. Maboudian, Lubrication of polycrystalline silicon MEMS via a thin silicon carbide coating, Sens. Actuators Phys. 193 (2013) 238–245. https://doi.org/10.1016/j.sna.2013.01.036.

[3] T. Frischmuth, M. Schneider, D. Maurer, T. Grille, U. Schmid, Inductively-coupled plasma-enhanced chemical vapour deposition of hydrogenated amorphous silicon carbide thin films for MEMS, Sens. Actuators Phys. 247 (2016) 647–655. https://doi.org/10.1016/j.sna.2016.05.042.

[4] A.K. Costa, S.S. Camargo, C.A. Achete, R. Carius, Characterization of ultra-hard silicon carbide coatings deposited by RF magnetron sputtering, Thin Solid Films. 377–378 (2000) 243–248. https://doi.org/10.1016/S0040-6090(00)01321-3.

[5] H. Habuka, M. Tsuji, Chemical vapor deposition of amorphous silicon carbide thin films on metal surfaces using monomethylsilane gas at low temperatures, Surf. Coat. Technol. 217 (2013) 88–93. https://doi.org/10.1016/j.surfcoat.2012.11.078.

[6] P.M. Sarro, Silicon carbide as a new MEMS technology, Sens. Actuators Phys. 82 (2000) 210–218. https://doi.org/10.1016/S0924-4247(99)00335-0.
[7] E.A. Filatova, D. Hausmann, S.D. Elliott, Understanding the Mechanism of SiC Plasma-Enhanced Chemical Vapor Deposition (PECVD) and Developing Routes toward SiC Atomic Layer Deposition (ALD) with Density Functional Theory, ACS Appl. Mater. Interfaces. 10 (2018) 15216–15225. https://doi.org/10.1021/acsami.8b00794.
[8] Z.D. Sha, X.M. Wu, L.J. Zhuge, Structure and photoluminescence properties of SiC films synthesized by the RF-magnetron sputtering technique, Vacuum. 79 (2005) 250–254. https://doi.org/10.1016/j.vacuum.2005.04.003.
[9] Q. Zhao, J.C. Li, H. Zhou, H. Wang, B. Wang, H. Yan, Parameters determining crystallinity in β-SiC thin films prepared by catalytic chemical vapor deposition, J. Cryst. Growth. 260 (2004) 176–180. https://doi.org/10.1016/j.jcrysgro.2003.08.026.
[10] W. Daves, A. Krauss, N. Behnel, V. Häublein, A. Bauer, L. Frey, Amorphous silicon carbide thin films (a-SiC:H) deposited by plasma-enhanced chemical vapor deposition as protective coatings for harsh environment applications, Thin Solid Films. 519 (2011) 5892–5898. https://doi.org/10.1016/j.tsf.2011.02.089.
[11] T.W. Scharf, J. Gong, G. Zangari, J.A. Barnard, Assessing defect density and wear resistance of ultrathin diamond-like carbon films, Appl. Phys. Mater. Sci. Process. 74 (2002) 827–829. https://doi.org/10.1007/s003390201286.
[12] K. Polychronopoulou, J. Lee, C. Tsotsos, N.G. Demas, R.L. Meschewski, C. Rebholz, A.A. Polycarpou, Deposition and Nanotribological Characterization of Sub-100-nm Thick Protective Ti-Based Coatings for Miniature Applications, Tribol. Lett. 44 (2011) 213–221. https://doi.org/10.1007/s11249-011-9839-x.
[13] Á. Barna, S. Gurban, L. Kotis, J. Lábár, A. Sulyok, A.L. Tóth, M. Menyhárd, J. Kovac, P. Panjan, Growth of amorphous SiC film on Si by means of ion beam induced mixing, Appl. Surf. Sci. 263 (2012) 367–372. https://doi.org/10.1016/j.apsusc.2012.09.063.
[14] G. Battistig, S. Gurbán, G. Sáfrán, A. Sulyok, A. Németh, P. Panjan, Z. Zolnai, M. Menyhárd, Wafer-scale SiC rich nano-coating layer by Ar + and Xe + ion mixing, Surf. Coat. Technol. 302 (2016) 320–326. https://doi.org/10.1016/j.surfcoat.2016.06.039.
[15] A.S. Racz, Z. Kerner, A. Nemeth, P. Panjan, L. Peter, A. Sulyok, G. Vertesy, Z. Zolnai, M. Menyhard, Corrosion Resistance of Nanosized Silicon Carbide-Rich Composite Coatings Produced by Noble Gas Ion Mixing, ACS Appl. Mater. Interfaces. 9 (2017) 44892–44899. https://doi.org/10.1021/acsami.7b14236.
[16] A.S. Racz, M. Menyhard, Design of Corrosion Resistive SiC Nanolayers, ACS Appl. Mater. Interfaces. 10 (2018) 22851–22856. https://doi.org/10.1021/acsami.8b06425.
[17] A.A. Tseng, C.-F.J. Kuo, S. Jou, S. Nishimura, J. Shirakashi, Scratch direction and threshold force in nanoscale scratching using atomic force microscopes, Appl. Surf. Sci. 257 (2011) 9243–9250. https://doi.org/10.1016/j.apsusc.2011.04.065.
[18] A. Wienss, G. Persch-Schuy, R. Hartmann, P. Joeris, U. Hartmann, Subnanometer scale tribological properties of nitrogen containing carbon coatings used in magnetic storage devices, J. Vac. Sci. Technol. Vac. Surf. Films. 18 (2000) 2023–2026. https://doi.org/10.1116/1.582466.
[19] A. Wienss, G. Persch-Schuy, M. Vogelgesang, U. Hartmann, Scratching resistance of diamond-like carbon coatings in the subnanometer regime, Appl. Phys. Lett. 75 (1999) 1077–1079. https://doi.org/10.1063/1.124602.
[20] M.-L. Wu, J.D. Kiely, T. Klemmer, Y.-T. Hsia, K. Howard, Process–property relationship of boron carbide thin films by magnetron sputtering, Thin Solid Films. 449 (2004) 120–124. https://doi.org/10.1016/S0040-6090(03)01464-0.

[21] B.D. Beake, M.I. Davies, T.W. Liskiewicz, V.M. Vishnyakov, S.R. Goodes, Nano-scratch, nanoindentation and fretting tests of 5–80nm ta-C films on Si(100), Wear. 301 (2013) 575–582. https://doi.org/10.1016/j.wear.2013.01.073.
[22] C. Tangpatjaroen, D. Grierson, S. Shannon, J.E. Jakes, I. Szlufarska, Size Dependence of Nanoscale Wear of Silicon Carbide, ACS Appl. Mater. Interfaces. 9 (2017) 1929–1940. https://doi.org/10.1021/acsami.6b13283.
[23] X. Li, Y. Wei, L. Lu, K. Lu, H. Gao, Dislocation nucleation governed softening and maximum strength in nano-twinned metals, Nature. 464 (2010) 877–880. https://doi.org/10.1038/nature08929.
[24] B.D. Beake, A.J. Harris, T.W. Liskiewicz, Review of recent progress in nanoscratch testing, Tribol. - Mater. Surf. Interfaces. 7 (2013) 87–96. https://doi.org/10.1179/1751584X13Y.0000000037.
[25] W.C. Oliver, G.M. Pharr, An improved technique for determining hardness and elastic modulus using load and displacement sensing indentation experiments, J. Mater. Res. 7 (1992) 1564–1583. https://doi.org/10.1557/JMR.1992.1564.
[26] A.A. Tseng, A comparison study of scratch and wear properties using atomic force microscopy, Appl. Surf. Sci. 256 (2010) 4246–4252. https://doi.org/10.1016/j.apsusc.2010.02.010.
[27] M. Menyhard, High-depth-resolution Auger depth profiling/atomic mixing, Micron. 30 (1999) 255–265. https://doi.org/10.1016/S0968-4328(99)00010-4.
[28] K.D. Childs, C.L. Hedberg, Physical Electronics, Incorporation, eds., Handbook of Auger electron spectroscopy: a book of reference data for identification and interpretation in Auger electron spectroscopy, 3. ed, Physical Electronics, Eden Prairie, 1995.
[29] L. Kotis, M. Menyhard, A. Sulyok, G. Sáfrán, A. Zalar, J. Kovač, P. Panjan, Determination of the relative sputtering yield of carbon to tantalum by means of Auger electron spectroscopy depth profiling, Surf. Interface Anal. 41 (2009) 799–803. https://doi.org/10.1002/sia.3101.
[30] S. Gurbán, L. Kotis, A. Pongracz, A. Sulyok, A.L. Tóth, E. Vázsonyi, M. Menyhard, The chemical resistance of nano-sized SiC rich composite coating, Surf. Coat. Technol. 261 (2015) 195–200. https://doi.org/10.1016/j.surfcoat.2014.11.032.
[31] D. Nečas, P. Klapetek, Gwyddion: an open-source software for SPM data analysis, Open Phys. 10 (2012). https://doi.org/10.2478/s11534-011-0096-2.
[32] SRIM Stopping and range of ions in matter by Ziegler, J. F. version SRIM, 2013 Software freely available www.srim.org., n.d. www.srim.org.
[33] R.J. Gaboriaud, C. Jaouen, J.J. Grob, A. Grob, Ion beam induced atomic mixing in Fe/Al bilayered samples, Appl. Phys. Solids Surf. 41 (1986) 127–135. https://doi.org/10.1007/BF00631120.
[34] V. Jardret, H. Zahouani, J.L. Loubet, T.G. Mathia, Understanding and quantification of elastic and plastic deformation during a scratch test, Wear. 218 (1998) 8–14. https://doi.org/10.1016/S0043-1648(98)00200-2.
[35] K.-H. Zum Gahr, Microstructure and wear of materials, Elsevier, Amsterdam; New York, 2010.
[36] J.F. Archard, Contact and Rubbing of Flat Surfaces, J. Appl. Phys. 24 (1953) 981–988. https://doi.org/10.1063/1.1721448.
[37] V. Kulikovsky, V. Vorlíček, P. Boháč, M. Stranyánek, R. Čtvrtlík, A. Kurdyumov, L. Jastrabik, Hardness and elastic modulus of amorphous and nanocrystalline SiC and Si films, Surf. Coat. Technol. 202 (2008) 1738–1745. https://doi.org/10.1016/j.surfcoat.2007.07.029.

[38] S. Sundararajan, B. Bhushan, Micro/nanotribological studies of polysilicon and SiC films for MEMS applications, Wear. 217 (1998) 251–261. https://doi.org/10.1016/S0043-1648(98)00169-0.

Graphical abstract:

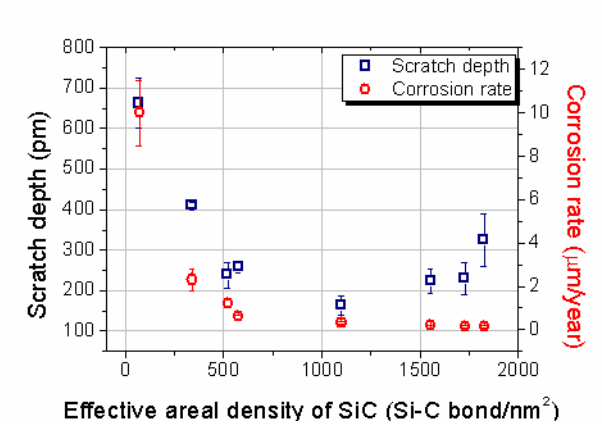

Declaration of competing interests

☒ The authors declare that they have no known competing financial interests or personal relationships that could have appeared to influence the work reported in this paper.

☐The authors declare the following financial interests/personal relationships which may be considered as potential competing interests:

Author statement

A.S. Racz: Conceptualization, Methodology, Investigation, Formal Analysis, Validation, Visualization, Writing – Original Draft, Review & Editing, Project administration, Funding acquisition, **D. Dworschak:** Resources, Writing - Review & Editing, **M. Valtiner:** Supervision, Methodology, Resources, Writing - Review & Editing, **M. Menyhard:** Supervision, Conceptualization, Visualization, Writing - Original Draft, Review & Editing

HIGHLIGHTS

- SiC-rich nano-layers were produced by ion beam mixing at room temperature.
- The scratch resistance correlated with the effective areal density of SiC.
- High effective areal density resulted in better scratch resistance than that of silicon.
- The scratch resistance of the samples correlated with the corrosion resistance.
- These findings allow the tailoring of the chemical and mechanical properties.

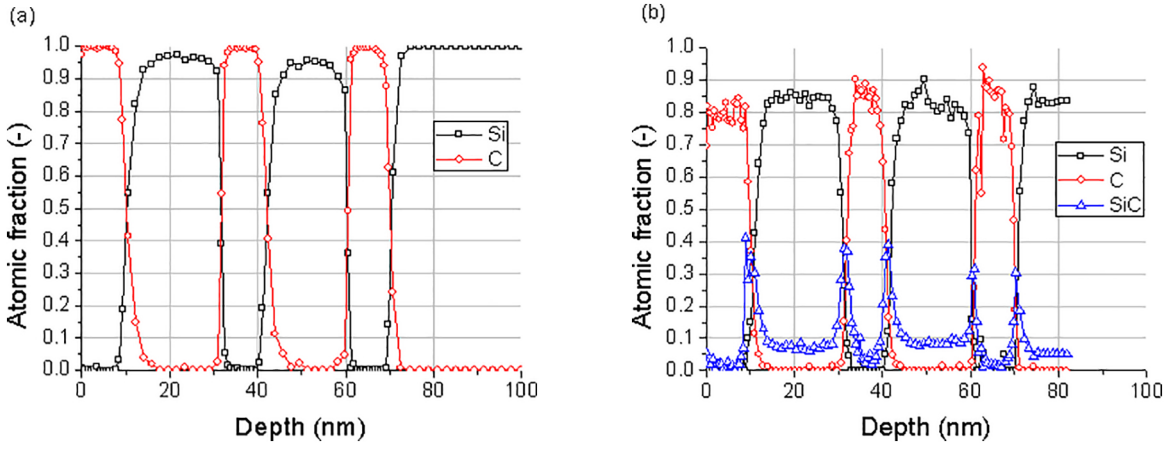
(a)
Atomic fraction (-)
Depth (nm)
Si
C
(b)
Atomic fraction (-)
Depth (nm)
Si
C
SiC

Figure 1

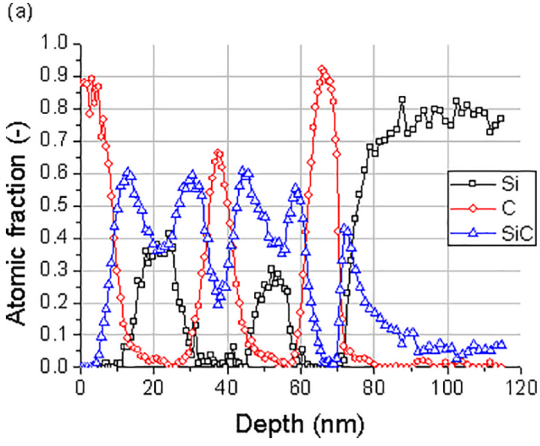
(a)
Atomic fraction (-)
Depth (nm)
Si
C
SiC
0.0
0.1
0.2
0.3
0.4
0.5
0.6
0.7
0.8
0.9
1.0
0
20
40
60
80
100
120

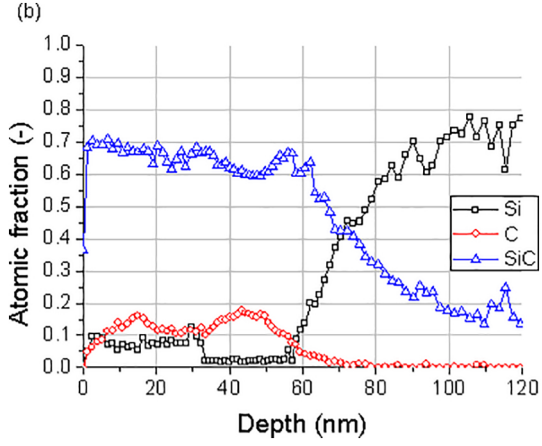
(b)
Atomic fraction (-)
Depth (nm)
Si
C
SiC
0.0
0.1
0.2
0.3
0.4
0.5
0.6
0.7
0.8
0.9
1.0
0
20
40
60
80
100
120

Figure 2

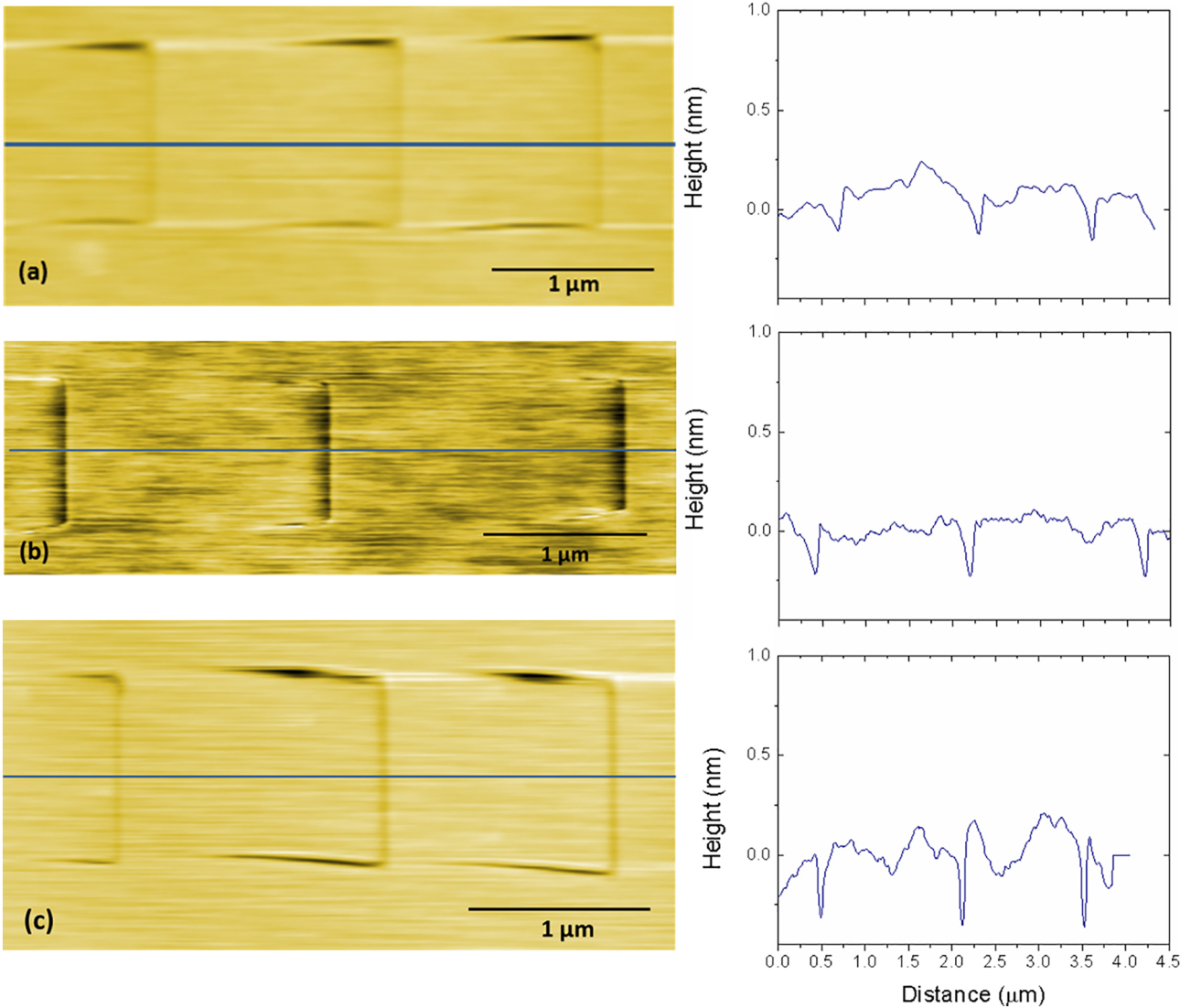
(a)
1 µm
(b)
1 µm
(c)
1 µm
Height (nm)
1.0
0.5
0.0
Height (nm)
1.0
0.5
0.0
Height (nm)
1.0
0.5
0.0
0.0 0.5 1.0 1.5 2.0 2.5 3.0 3.5 4.0 4.5
Distance (µm)

Figure 3

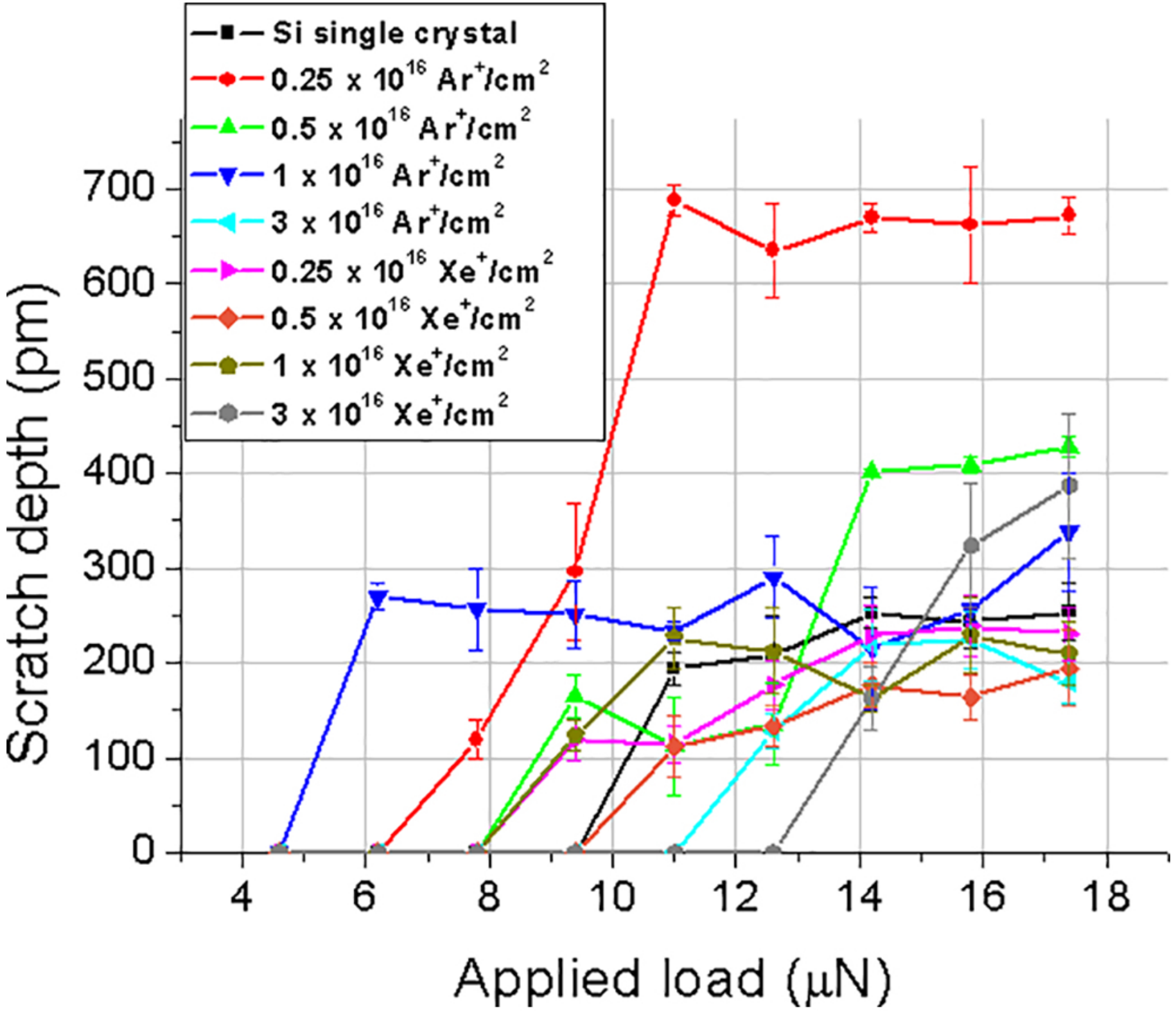
Si single crystal
0.25 x 10^16 Ar+/cm2
0.5 x 10^16 Ar+/cm2
1 x 10^16 Ar+/cm2
3 x 10^16 Ar+/cm2
0.25 x 10^16 Xe+/cm2
0.5 x 10^16 Xe+/cm2
1 x 10^16 Xe+/cm2
3 x 10^16 Xe+/cm2
Scratch depth (pm)
0
100
200
300
400
500
600
700
4
6
8
10
12
14
16
18
Applied load (μN)

Figure 4

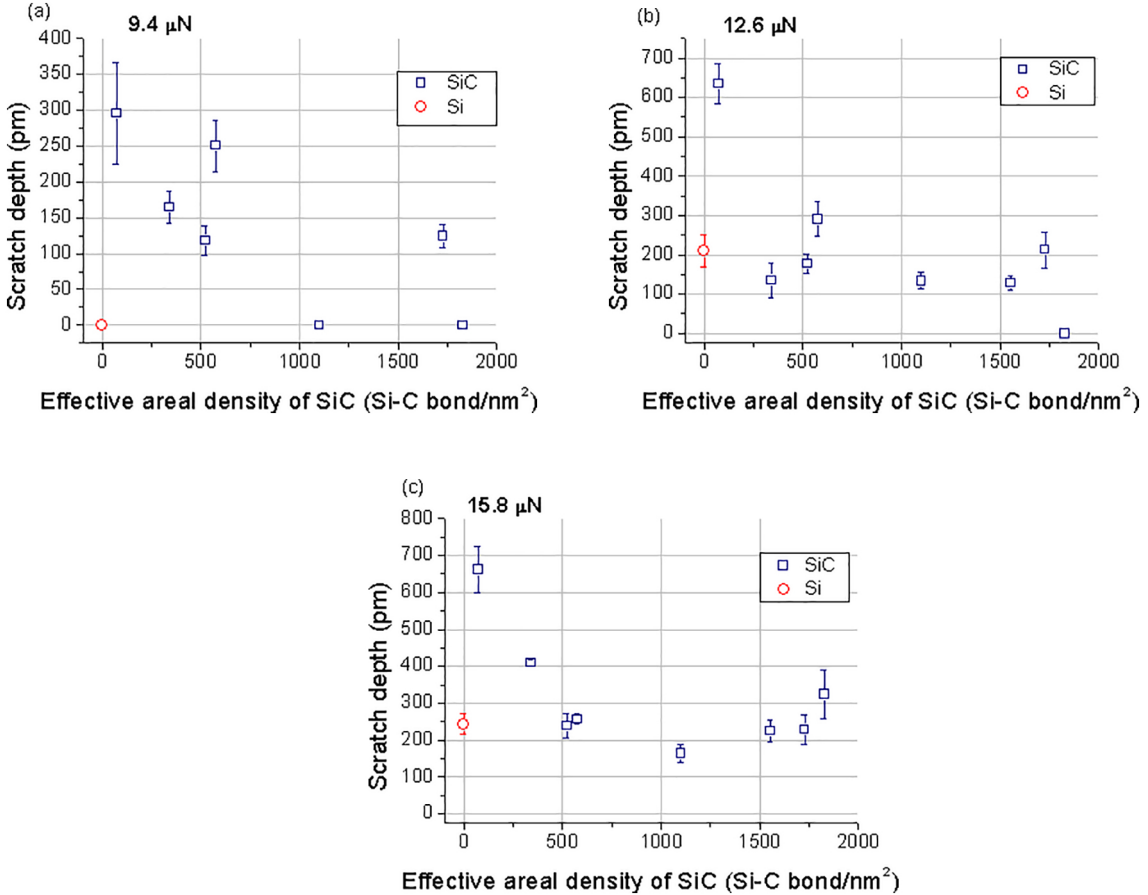
(a)
9.4 μN
Scratch depth (pm)
Effective areal density of SiC (Si-C bond/nm^2)
SiC
Si
(b)
12.6 μN
Scratch depth (pm)
Effective areal density of SiC (Si-C bond/nm^2)
SiC
Si
(c)
15.8 μN
Scratch depth (pm)
Effective areal density of SiC (Si-C bond/nm^2)
SiC
Si

Figure 5

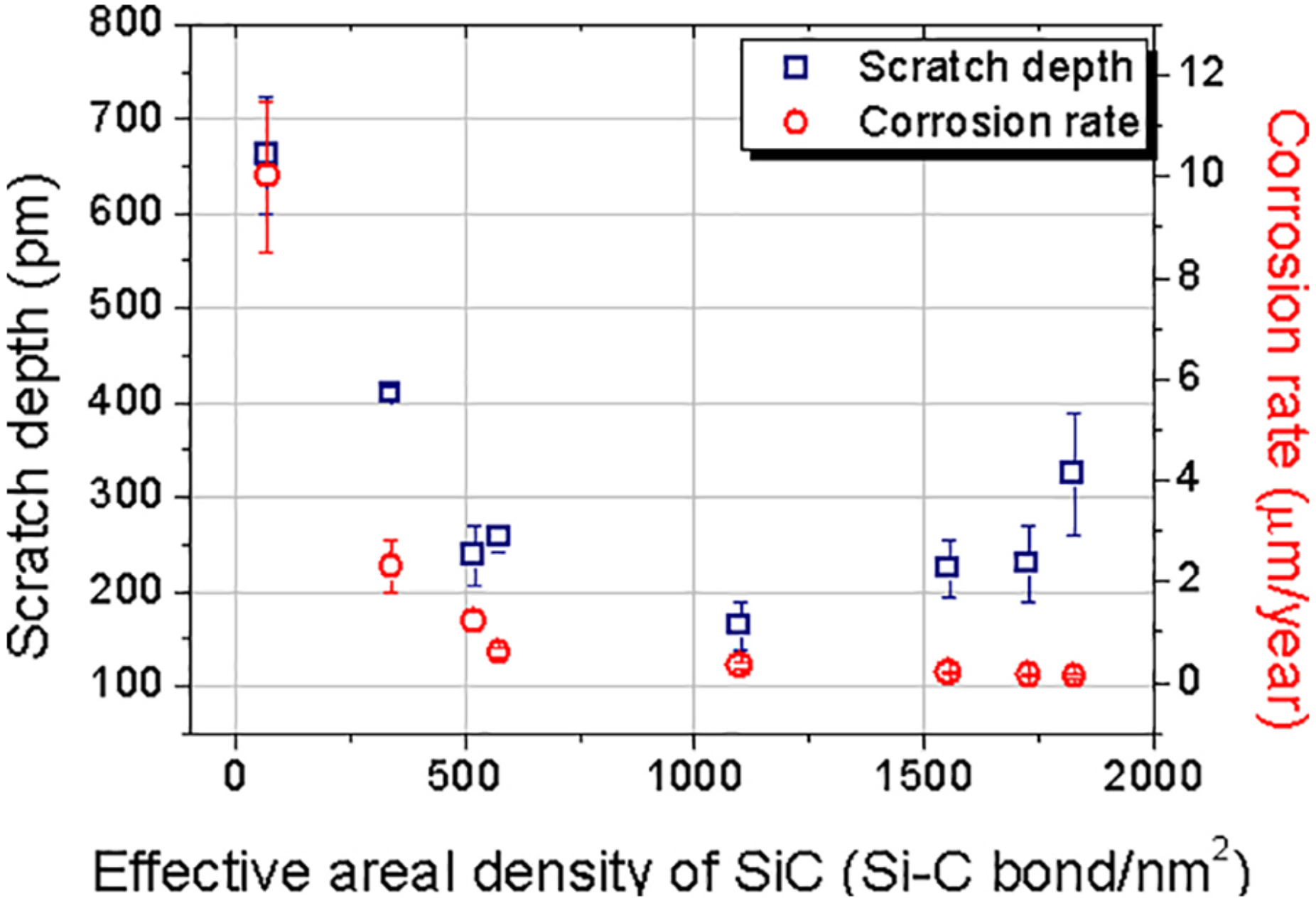
Scratch depth
Corrosion rate
Scratch depth (pm)
Corrosion rate (μm/year)
Effective areal density of SiC (Si-C bond/nm²)
800
700
600
500
400
300
200
100
12
10
8
6
4
2
0
0
500
1000
1500
2000

Figure 6